Inorg. Chem. **1988**, *27*, 2801–2804 **2801**

Contribution from the Department of Chemistry,
University of Hong Kong, Pokfulam Road, Hong Kong

Synthesis, Reactivity, and X-ray Structural Characterization of *trans*-Dioxoosmium(VI) Porphyrin Complexes

Chi-Ming Che,* Wai-Cheung Chung, and Ting-Fong Lai*

Received February 3, 1988

The oxidation of [Os(P)(CO)(EtOH)] (P = porphyrin dianion) to $[Os(P)(O)_2]$ by *m*-chloroperoxybenzoic acid in CH_2Cl_2 proceeds through a stable Os(IV) intermediate. The $[Os(p\text{-}X\text{-}TPP)(O)_2]$ (X = Cl, H, OMe, Me) and $[Os(TMP)(O)_2]$ complexes have been characterized by UV–vis, ^1H NMR, and IR spectroscopy. The crystal structure of $[Os(p\text{-}Me\text{-}TPP)(O)_2]\cdot 2C_4H_8O$ ($H_2(p\text{-}Me\text{-}TPP)$ = *meso*-tetra-*p*-tolylporphyrin) has been determined: monoclinic, space group $P2_1/c$, $a = 11.025$ (1) Å, $b = 16.977$ (2) Å, $c = 13.196$ (2) Å, $\beta = 110.21$ (1)°, $Z = 2$. The Os–porphinato unit is planar with Os–N = 2.066 (4) Å and Os–O = 1.743 (3) Å. The $[Os(P)(O)_2]$ complexes are ineffective in the epoxidation of olefins. Stirring $[Os(TPP)(O)_2]$ and $[Os(TMP)(O)_2]$ wtih cyclohexene at 52 °C yielded cyclohexenol.

Introduction

There is a growing interest in the oxidation chemistry of oxo–ruthenium and –osmium complexes, which are potential catalysts for aerobic and selective oxidative reactions.[1–6] Groves and co-workers recently reported a *trans*-dioxoruthenium(VI) porphyrin complex, $[Ru(TMP)(O)_2]$ (H_2TMP = tetramesitylporphyrin), which is capable of catalyzing aerobic epoxidation of olefins.[5] Their work has initiated our interest in the oxidation of chemistry of this ruthenium system. However, attempts to structurally characterize $[Ru(TMP)(O)_2]$ have so far been unsuccessful, and we have found that this Ru(VI) complex easily undergoes unknown degradation reactions both in the solid state and in fluid solution.[5,7] We believe that knowledge of the structure and reactivities of the isoelectronic *trans*-dioxoosmium(VI) porphyrin complexes ($[Os(P)(O)_2]$, P = porphyrin dianion), which should be kinetically more inert than their ruthenium analogues, will be useful in elucidating the complex chemistry of $[Ru(TMP)(O)_2]$. In this contribution, a study of the oxidation of [Os(P)(CO)] to $[Os(P)(O)_2]$ by *m*-chloroperoxyybenzoic acid (*m*-CPBA) and the x-ray structure of $[Os(p\text{-}Me\text{-}TPP)(O)_2]$ ($H_2(p\text{-}Me\text{-}TPP)$ = *meso*-tetra-*p*-tolylporphyrin) are described.

Experimental Section

Materials. Octaethylporphyrin (H_2OEP) and dodecacarbonylosmium ($Os_3(CO)_{12}$) were purchased from Strem Co. Ltd. All solvents and chemicals in syntheses are analytical grade. The [Os(P)(CO)(EtOH)] complexes were prepared by refluxing $Os_3(CO)_{12}$ and H_2P in diethylene glycol monomethyl ether under nitrogen atmosphere;[8] details of their spectroscopic and electrochemical properties will be reported later.

Abbreviations used for the $[Os(P)(O)_2]$ porphyrins are as follows. H_2P: $H_2(p\text{-}MeO\text{-}TPP)$, *meso*-tetrakis(*p*-methoxyphenyl)porphyrin; $H_2(p\text{-}Me\text{-}TPP)$, *meso*-tetra-*p*-tolylporphyrin; $H_2(p\text{-}Cl\text{-}TPP)$, *meso*-tetrakis(*p*-chlorophenyl)porphyrin); H_2TPP, *meso*-tetraphenylporphyrin.

[Os(P)(CO)(EtOH)] (100 mg) and *tert*-butyl hydroperoxide (TBHP, 2 mL) were stirred in CH_2Cl_2/EtOH solution (1:1, 50 mL) at room temperature for 2 h. After reaction was completed, the solvent was evaporated to ~10 mL. A violet-black crystalline solid gradually deposited upon standing and was purified by chromatography on a silica gel column with $CH_2Cl_2/(CH_3)_2CO$ (10:1) solution as the eluent. Overall yields varied from 60% to 80%.

Alternatively, [Os(P)(CO)(EtOH)] (100 mg) and *m*-chloroperoxybenzoic acid (50 mg) were stirred in CH_2Cl_2 (50 mL) at room temperature for $^1/_2$ h. The solution was then evaporated to ~2 mL and chromatographed on a silica gel column with $CHCl_3$ as the eluent. Yield was ~70%. The $[Os(P)(O)_2]$ complexes can be recrystallized in CH_2Cl_2/CH_3CN (1:1) or CH_2Cl_2/C_4H_8O solution.

Anal. Calcd for $[Os(p\text{-}MeO\text{-}TPP)(O)_2]$: C, 60.4; H, 3.8; N, 5.9. Found: C, 60.1; H, 3.9; N, 5.7. Calcd for $[Os(p\text{-}Cl\text{-}TPP)(O)_2]$: C, 54.3; H, 2.5; N, 5.7; Cl, 14.6. Found: C, 54.3; H, 2.7; N, 5.4; Cl, 14.7. Calcd for $[Os(TPP)(O)_2]$: C, 63.3; H, 3.4; N, 6.7. Found: C, 62.9; H, 3.5; N, 6.4. Calcd for $[Os(p\text{-}Me\text{-}TPP)(O)_2]\cdot 2C_4H_8O$: C, 67.8; H, 5.1; N, 5.5. Found: C, 67.6; H, 5.0, N, 5.4.

$[Os(TMP)(O)_2]$. [Os(TMP)(CO)(EtOH)] (120 mg) was dissolved in CH_2Cl_2/EtOH solution (1:1, 50 mL), and the mixture was treated with hydrogen peroxide (0.5 mL). The solution was then refluxed for $^1/_2$ h. After refluxing, the solution was evaporated to dryness. The crude solid was purified by chromatography on a silica gel column with $CHCl_3$ as the eluent. Pure $[Os(TMP)(O)_2]$ was obtained by recrystallization of the sample from CH_2Cl_2/CH_3CN (1:2) solution. Yield was ~70%. Anal. Calcd for $[Os(TMP)(O)_2]\cdot 2CH_2Cl_2$: C, 59.4; H, 4.8; N, 4.8. Found: C, 59.3; H, 4.9; N, 4.8.

Reaction of $[Os(OEP)(O)_2]$ with L-(±)-Ascorbic Acid. $[Os(OEP)(O)_2]$ (100 mg) and L-(+)-ascorbic acid (2 g) in CH_3CN/H_2O (5:1, 50 mL) solution were stirred at 50–60 °C for 2 h. When all $[Os(OEP)(O)_2]$ had reacted, the solution was evaporated to remove CH_3CN. An aqueous suspension of $[Os(OEP)(OH)_2]$ remained and was filtered. The osmium product was washed with water and dried under vacuum. The IR spectrum of a freshly prepared sample of $[Os(OEP)(OH)_2]$ exhibits an intense and broad ν(O–H) stretch at ~3650 cm^{-1}. Attempts to obtain a pure sample of $[Os(OEP)(OH)_2]$ have been unsuccessful, since it is easily air-oxidized back to $[Os(OEP)(O)_2]$.

Oxidation of Organic Substrates by $[Os(P)(O)_2]$. Exactly weighed amounts of the $[Os(P)(O)_2]$ complex and cyclohexane (~3–4 mL) were stirred at constant temperature for 20 h. The organic products were analyzed by gas chromatography and mass spectroscopy.

Physical Measurements. UV–vis spectra were recorded on a Shimadzu UV-250 spectrophotometer. ^1H NMR spectra were run on a JEOL Model FX90Q Fourier transform NMR spectrometer (90 MHz), with tetramethylsilane as an internal standard.

X-ray Crystal Structure of $[Os(p\text{-}Me\text{-}TPP)(O)_2]\cdot 2C_4H_8O$. Crystals of $[Os(p\text{-}Me\text{-}TPP)(O)_2]\cdot 2C_4H_8O$ were obtained by slow evaporation of a dichloromethane/tetrahydrofuran (C_4H_8O) solution of $[Os(p\text{-}Me\text{-}TPP)(O)_2]$ at room temperature. The crystals are air stable.

X-ray diffraction data were collected on an Enraf-Nonius CAD4 diffractometer with graphite-monochromated Mo Kα radiation (λ = 0.71073 Å). The unit cell dimensions were obtained from a least-squares fit of 25 reflections in the region of $29° \leq 2\theta < 37°$. The data were corrected for Lorentz, polarization, and absorption effects. The empirical absorption correction was based on azimuthal (ψ) scans of six reflections with $80 < \chi < 90°$. Three check reflections, monitored every 2 h, showed a gradual decrease in intensity of about 3% during the 120 h of X-ray exposure. Crystal and structure determination data are summarized in Table I. Calculations were carried out on a MICROVAX II computer using the Enraf-Nonius SDP.[9]

---

(1) (a) Che, C. M.; Leung, W. H.; Poon, C. K. *J. Chem. Soc., Chem. Commun.* **1987**, 173. (b) Che, C. M.; Lai, T. F.; Wong, K. Y. *Inorg. Chem.* **1987**, *26*, 2289. (c) Che, C. M.; Leung, W. H. *J. Chem. Soc., Chem. Commun.* **1987**, 1376. (d) Che, C. M.; Cheng, W. .; Mak, T. C. W. *J. Chem. Soc., Chem. Commun.* **1986**, 200. (e) Che, C. M.; Wong, K. Y.; Leung, W. H.; Poon, C. K. *Inorg. Chem.* **1986**, *25*, 345. (f) Che, C. M.; Chung, W. C. *J. Chem. Soc., Chem. Commun.* **1986**, 386.

(2) Bailey, C. L.; Drago, R. S. *J. Chem. Soc., Chem. Commun.* **1987**, 179.

(3) Lau, T. C.; Kochi, J. K. *J. Chem. Soc., Chem. Commun.* **1987**, 798.

(4) Marmion, M. E.; Takeuchi, K. J. *J. Chem. Soc., Chem. Commun.* **1987**, 1396.

(5) (a) Groves, J. T.; Quinn, R. *J. Am. Chem. Soc.* **1985**, *107*, 5790. (b) Groves, J. T.; Quinn, R. *Inorg. Chem.* **1984**, *23*, 3844.

(6) (a) Pipes, D. W.; Meyer, T. J. *Inorg. Chem.* **1986**, *25*, 4043. (b) Roecker, L.; Meyer, T. J. *J. Am. Chem. Soc.* **1986**, *108*, 4066 and references therein. (c) Dobson, J. C.; Takeuchi, K. J.; Pipes, D. W.; Geselowitz, D. A.; Meyer, T. J. *Inorg. Chem.* **1986**, *25*, 2357.

(7) Che, C. M.; Yeung, C. H., unpublished results.

(8) Che, C. M.; Poon, C. K.; Chung, W. C.; Gray, H. B. *Inorg. Chem.* **1985**, *24*, 1277.

(9) "Enraf-Nonius Structure Determination Package, SDP"; Enraf-Nonius: Delft, The Netherlands, 1985.

0020-1669/88/1327-2801$01.50/0 © 1988 American Chemical Society

Table I. Crystal Data and Summary of Data Collection and Refinement

formula	$C_{48}H_{36}N_4O_2Os{\cdot}2C_4H_8O$
fw	1035.26
space group	$P2_1/c$
a, Å	11.025 (1)
b, Å	16.977 (2)
c, Å	13.196 (2)
β, deg	110.21 (1)
V, Å^3	2317.8 (9)
Z	2
$F(000)$	1048
d_{calcd}, g cm^{-3}	1.482
d_{mesd}, g cm^{-3}	1.48
cryst size, mm	0.47, 0.28, 0.25
μ(Mo Kα), cm^{-1}	28.03
scan type; scan speed, deg min^{-1}	ω–2θ; 1.2–5.5
scan width, deg	0.8 + 0.34 tan θ
background	25% of full scan width on both sides
temp, K	298
collection range	$2\theta_{max}$ = 54°; $\pm h,k,\pm l$
transmission factor	0.929–0.999
no. of reflcns measd	9495
no. of independent reflcns	4740
no. of reflcns used in calcns, m	3379 [$I > 1.5\sigma(I)$]
no. of params refined, p	270
R[a]	0.030
R_w[a]	0.047
goodness of fit[a]	1.73

[a] $R = \sum||F_o| - |F_c||/\sum|F_o|$. $R_w = [\sum w(|F_o| - |F_c|)^2/\sum w|F_o|^2]^{1/2}$, with $w = 4F_o^2/[\sigma^2(F_o^2) + (0.04F_o^2)^2]$. Goodness of fit = $[\sum w(|F_o| - |F_c|)^2/(m - p)]^{1/2}$.

Table II. Atomic Coordinates for Non-Hydrogen Atoms in [Os(p-Me-TPP)(O)$_2$] (×10^4) and in Tetrahydrofuran (×10^3) with Esd's in Parentheses

atom	x	y	z	B_{eq}, Å^2
Os	0	0	0	2.860 (4)
O	1240 (4)	−76 (2)	1247 (3)	3.93 (8)
N(1)	−780 (3)	−1053 (2)	264 (3)	3.28 (7)
N(2)	−1123 (3)	597 (2)	719 (3)	3.36 (8)
C(1)	−1722 (4)	−1136 (3)	718 (4)	3.6 (1)
C(2)	−2270 (4)	−543 (3)	1128 (4)	3.7 (1)
C(3)	−1994 (4)	265 (3)	1123 (4)	3.7 (1)
C(4)	−2586 (4)	888 (3)	1522 (4)	4.3 (1)
C(5)	−2114 (4)	1569 (3)	1317 (4)	4.3 (1)
C(6)	−1185 (4)	1402 (3)	809 (4)	3.5 (1)
C(7)	−488 (4)	1954 (3)	462 (4)	3.5 (1)
C(8)	−452 (5)	−1781 (3)	24 (4)	3.7 (1)
C(9)	−1261 (4)	−2353 (3)	283 (4)	4.2 (1)
C(10)	−2014 (4)	−1966 (3)	715 (4)	4.2 (1)
C(11)	−3286 (4)	−774 (3)	1601 (4)	3.8 (1)
C(12)	−2964 (5)	−924 (4)	2689 (4)	5.2 (1)
C(13)	−3875 (5)	−1128 (4)	3111 (5)	6.6 (2)
C(14)	−5189 (5)	−1214 (4)	2449 (5)	5.5 (1)
C(15)	−5481 (5)	−1066 (5)	1370 (5)	7.2 (2)
C(16)	−4564 (5)	−863 (5)	944 (5)	6.6 (2)
C(17)	−6205 (6)	−1466 (5)	2923 (5)	8.3 (2)
C(18)	−726 (4)	2815 (3)	600 (4)	3.8 (1)
C(19)	−1257 (6)	3300 (3)	−291 (4)	5.7 (2)
C(20)	−1449 (6)	4077 (4)	−175 (5)	6.4 (3)
C(21)	−1167 (5)	4409 (3)	828 (5)	5.2 (1)
C(22)	−680 (5)	3930 (3)	1726 (5)	4.9 (1)
C(23)	−467 (5)	3148 (3)	1604 (4)	4.5 (1)
C(24)	−1415 (9)	5330 (4)	955 (7)	9.8 (3)
C(31)	413 (1)	361 (1)	698 (1)	13.4 (3)[a]
C(32)	311 (1)	334 (1)	757 (1)	14.1 (4)[a]
C(33)	406 (1)	339 (1)	884 (1)	14.4 (4)[a]
C(34)	485 (1)	411 (1)	888 (1)	19.1 (5)[a]
C(35)	511 (2)	376 (2)	795 (2)	31 (1)[a]

[a] Atom in THF with isotropic thermal parameter.

Table III. Selected Distances (Å) and Angles (deg) for [Os(p-Me-TPP)(O)$_2$]

Os–O	1.743 (3)	O–Os–N(1)	90.7 (1)
Os–N(1)	2.065 (4)	O–Os–N(2)	90.2 (2)
Os–N(2)	2.067 (4)	N(1)–Os–N(2)	89.8 (2)

Table IV. Characteristic $\nu_{as}(OsO_2)$ Stretches of [Os(P)(O)$_2$]

complex	$\nu_{as}(OsO_2)$, cm^{-1} [a]
[Os(TMP)(O)$_2$]	841
[Os(p-MeO-TPP)(O)$_2$]	841
[Os(p-Me-TPP)(O)$_2$]	843
[Os(TPP)(O)$_2$]	845, 833
[Os(p-Cl-TPP)(O)$_2$]	841
[Os(MIX-DME)(O)$_2$][b]	839

[a] In Nujol mull. [b] H_2(MIX-DME) = mesoporphyrin IX dimethyl ester; ref 9.

The structure was solved by placing the Os atom on the inversion center at 0, 0, 0 and calculating a series of Fourier maps to locate all the non-hydrogen atoms. Refinement was by full-matrix least squares. The non-hydrogen atoms in [Os(p-Me-TPP)(O)$_2$] were refined with anisotropic thermal parameters, while those in the tetrahydrofuran molecule were refined with isotropic thermal parameters. Since the tetrahydrofuran molecule was disordered with large thermal motion, no attempt was made to locate the oxygen atom and all the atoms were assigned as carbon. Such a disorder involving carbon and oxygen atoms seems to be due to the fact that no cation is present to orient the oxygen. The hydrogen atoms were included at their calculated positions (C–H = 0.95 Å) and were given thermal parameters 1.1 times the equivalent isotropic thermal parameter of the bonded carbon atom. Hydrogen atoms in the methyl groups and also those in tetrahydrofuran were omitted. The final difference Fourier map was essentially featureless except for some peaks (<1 e/Å^3) in the region of the solvent molecule, clearly affected by disorder.

Final agreement factors are shown in Table I. Atomic parameters of non-hydrogen atoms are listed in Table II. Selected bond distances and angles are given in Table III. Tables of calculated hydrogen atomic coordinates, anisotropic thermal parameters, and structure factors are available as supplementary material.

Results and Discussion

Most [Os(P)(O)$_2$] complexes are conveniently prepared by oxidation of [Os(P)(CO)] with TBHP or m-CPBA.[8,10] However, the oxidation of [Os(TMP)(CO)(EtOH)] to [Os(TMP)(O)$_2$], which has the sterically hindered porphinato ligand, requires drastic conditions, involving the reaction with H_2O_2 at ~70–80 °C.

Groves and co-workers reported that oxidation of [Ru(TMP)(CO)] with m-CPBA in CH_2Cl_2 affords [Ru(TMP)(O)$_2$] without an observable intermediate.[5b] These workers suggested that the oxidation may proceed through the formation of an unstable oxoruthenium(IV) complex, which rapidly disproportionates into Ru(II) and Ru(VI).[6b] In this work, it has been found that oxidation of [Os(P)(CO)] with m-CPBA yields stable Os(IV) species, which subsequently transform into [Os(P)(O)$_2$]. Figure 1a shows the visible spectral changes during the course of reaction for [Os(OEP)(O)(EtOH)] in CH_2Cl_2. Upon addition of m-CPBA (in excess of [Os(OEP)(CO)(EtOH)]), a new species I, having essentially the same optical spectrum at [Os(OEP)(OR)$_2$][8,11] (R = Me, Et) Figure 1b), was immediately formed and then slowly transformed into [Os(OEP)(O)$_2$] as the final product (Figure 1). The same complex I, which exhibits an intense and broad IR band at ~3650 cm^{-1}, could also be prepared by reduction of [Os(OEP)(O)$_2$] with ascorbic acid in CH_3CN/H_2O (5:1) soluiton at ~50 °C (see Experimental Section). Since ascorbic acid reduction of [Os(OEP)(O)$_2$] or [Os(TPP)(O)$_2$] in ROH yields [Os(OEP)(OR)$_2$] or [Os(TPP)(OR)$_2$] quantitatively,[12] complex I is an Os(IV) complex and likely to be [Os(OEP)(OH)$_2$], which is expected to have an optical spectrum similar to that of [Os(OEP)(OR)$_2$].[2] The oxidation of [Os(OEP)(OH)$_2$] (I) to [Os(OEP)(O)$_2$] by m-CPBA is a clean reaction, as evidenced by the

---

(10) Buchler, J. W.; Smith, P. D. *Angew. Chem., Int. Ed. Engl.* **19** 74, *13*, 341.

(11) (a) Buchler, J. W.; Smith, P. D. *Chem. Ber.* **1976**, *109*, 1465. (b) Buchler, J. W.; Herget, G.; Oesten, K. *Liebigs Ann. Chem.* **1983**, 2164.

(12) Chung, W. C. Ph.D. Thesis, University of Hong Kong, 1987.

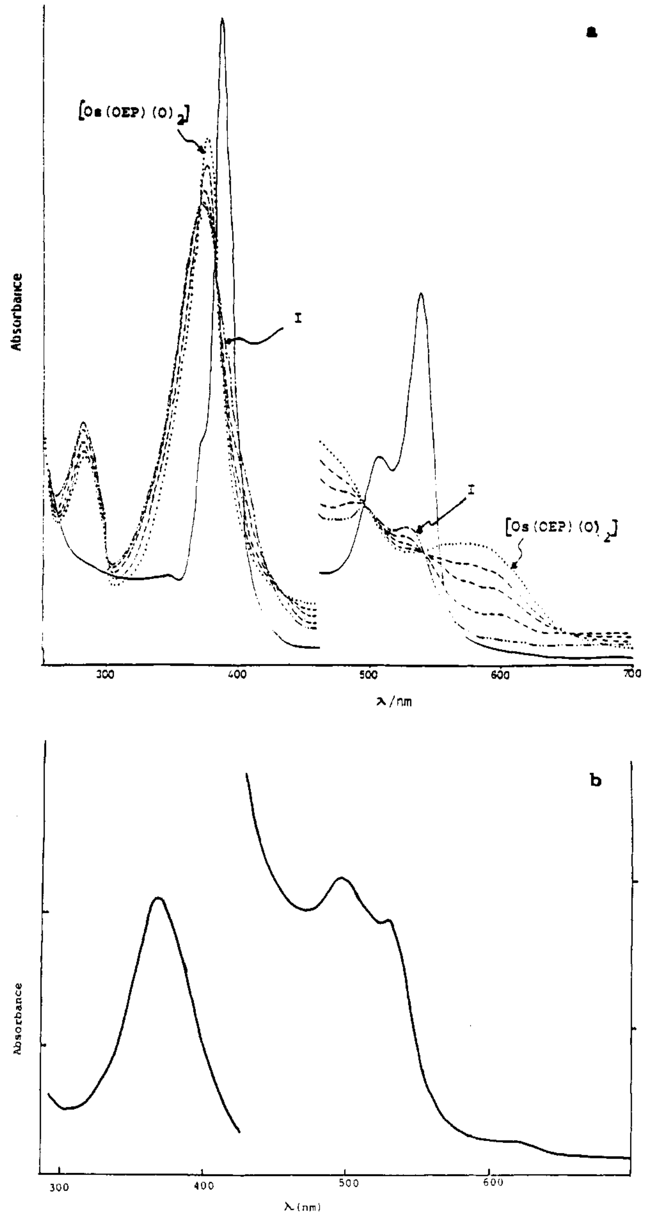

Figure 1. (a) UV-vis spectral changes for the oxidation of [Os(OEP)(CO)(EtOH)] to [Os(OEP)(O)$_2$] in CH$_2$Cl$_2$ by *m*-CPBA. (b) UV-vis spectrum of [Os(OEP)(OEt)$_2$].

Table V. ^{1}H NMR Spectral Data (90 MHz) for the [Os(P)(O)$_2$] Complexes

	chem shifts, ppm (referenced to Me$_4$Si)			
complex	pyrrolic CH	*o*-H[a]	*m*-H[a]	*p*-X[a]
[Os(*p*-MeO-TPP)(O)$_2$]	9.15 (s)	8.26 (d)	7.35 (d)	4.13 (s)
[Os(*p*-Me-TPP)(O)$_2$]	9.14 (s)	8.23 (d)	7.72 (d)	2.73 (s)
[Os(TPP)(O)$_2$]	9.13 (s)	8.36 (dd)	7.83 (m)	
[Os(*p*-Cl-TPP)(O)$_2$]	9.13 (s)	8.27 (d)	7.81 (d)	
[Os(TMP)(O)$_2$]	8.86 (s)	1.89 (s, CH$_3$)[b]	7.31 (s)	2.64 (s)

[a] Proton signals of the phenyl ring; *p*-X refers to the para substituents. [b] The 1.89 ppm signal refers to the *o*-CH$_3$ protons of the TMP ligand.

Table VI. UV-Vis Spectral Data for the [Os(P)(O)$_2$] Complexes in CH$_2$Cl$_2$

complex	λ_{max}, nm (log ϵ)
[Os(TPP)(O)$_2$]	586 (3.71), 479 sh (4.08), 395 (4.82), 339 (4.15)
[Os(*p*-MeO-TPP)(O)$_2$]	590 (3.75), 477 sh (4.18), 400 (4.80), 330 (4.22)
[Os(*p*-Me-TPP)(O)$_2$]	585 (3.74), 460 sh (4.10), 396 (4.80), 332 (4.20)
[Os(*p*-Cl-TPP)(O)$_2$]	581 (3.79), 463 sh (4.23), 396 (4.88), 338 (4.25)
[Os(TMP)(O)$_2$]	585 (4.09), 458 sh (4.52), 393 (5.09), 355 (4.48), 310 (4.40)

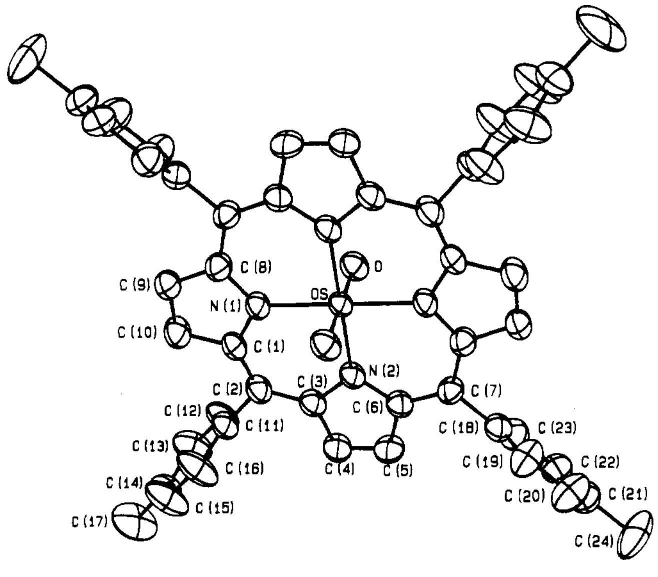

Figure 2. ORTEP drawing of [Os(*p*-Me-TPP)(O)$_2$] with the atomic numbering scheme.

isosbestic points in Figure 1a. In contrast to [Ru^{IV}(TMP)(O)], the [Os(OEP)(OH)$_2$] complex does not appear to undergo disproportionation in solution at room temperature.

The [Os(*p*-X-TPP)(O)$_2$] (X = Cl, Me, OMe) and [Os(TMP)(O)$_2$] complexes are air-stable diamagnetic solids; their spectral data are tabulated in Tables IV–VI. The ν_{as}(OsO$_2$) stretches range from 840 to 843 cm^{-1}, which are at a higher frequency than that for the ν_{as}(RuO$_2$) stretch (821 cm^{-1}) of [Ru(TMP)(O)$_2$].[5] Considering the higher atomic mass of osmium compared to ruthenium, the IR spectral data indicate a stronger metal–oxo bond for the [Os(P)(O)$_2$] system. The ^{1}H NMR spectrum of [Os(*p*-X-TPP)(O)$_2$] in the aromatic region (δ = 7–9) shows an AB quartet or two pseudodoublets at 8.23–8.27 and 7.35–7.81 ppm. The observed splitting is ~8 Hz, which approximates well to the ortho-coupling constants of aromatic protons. The signals at 8.23–8.27 ppm, which are absent in [Os(TMP)(O)$_2$], are logically assigned to be the ortho protons of the phenyl rings. The structure of [Os(*p*-Me-TPP)(O)$_2$], a prototype for the [Os(*p*-X-TPP)(O)$_2$] and [Os(TMP)(O)$_2$] systems, has been established by X-ray crystallography. Figure 2 shows an ORTEP drawing of [Os(*p*-Me-TPP)(O)$_2$] with the atomic numbering scheme. This is the first example of the structure of a *trans*-dioxo(porphinato)metal complex. The *trans*-osmyl moiety [Os(O)$_2$] is linear and almost perpendicular to the equatorial porphinato ring (angle between the Os–O line and the least-squares plane of the ring is 88.35 (7)°). The measured osmyl Os–O distance of 1.743 (3) Å corresponds to a short and strong metal–oxo bond. When compared with those of *trans*-[Os(en)$_2$O$_2$]$^{2+}$ (d(Os=O) = 1.74 (1) Å)[13] and [Os(3-*t*-Bu-saltmen)(O)$_2$] (d(Os=O) = 1.722 (8) and 1.760 (7) Å),[14] the Os–O bond lengths are seen to be similar despite the dramatic variation in the structure of the equatorial ligands. This is in contrast to the bond lengths in the oxoruthenium(IV) system, where replacing the saturated tertiary amine by a π-aromatic amine results in a significant lengthening of the Ru=O bond. [d(Ru=O) values for *trans*-[Ru^{IV}(TMC)O(Cl)]$^+$ and *trans*-[Ru^{IV}(py)$_4$O(Cl)]$^+$ are 1.765 (5) and 1.862 (8) Å, respectively].[1b,15] The average Os–N distance is 2.066 (4) Å, similar to values found in other osmium porphyrin

---

(13) Malin, J. M.; Schlemper, E. O.; Murmann, R. K. *Inorg. Chem.* **1977**, *16*, 615.

(14) Che, C. M.; Cheng, W. K.; Mak, T. C. W. *Inorg. Chem.* **1988**, *27*, 250.

(15) Yukawa, Y.; Aoyagi, K.; Kurihara, M.; Shirai, K.; Shimiza, K.; Mukaida, M.; Takeuchi, T.; Kakihana, H. *Chem. Lett.* **1985**, 283.

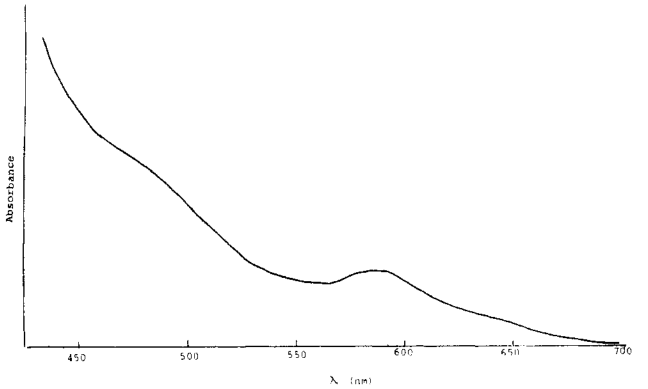

Figure 3. UV–vis spectrum of $[\mathrm{Os(TMP)(O)_2}]$ in $\mathrm{CH_2Cl_2}$.

Table VII. Oxidation of Cyclohexene by $[\mathrm{Os(P)(O)_2}]$ at 52 °C under Aerobic Conditions

complex	10^5 × amt of Os complex used, mL	10^5 × amt of cyclohexenol formed, mol	no. of equiv
$[\mathrm{Os(TPP)(O)_2}]$	3.0	7.6	2.5
$[\mathrm{Os(TMP)(O)_2}]$	1.7	5.5	3.2

complexes $[\mathrm{Os(TPP)(PPh_3)_2}$, 2.044 (2); $\mathrm{Os(OEP)(OPPh_3)_2}$, 2.029 (8); $\mathrm{Os(Me_2OEP)(CO)(py)}$, 2.067 (3) Å].[16,17] The porphyrin skeleton is approximately planar. Deviations from the least-squares plane of the core atoms vary from 0.007 to 0.070 Å (rms displacement 0.036 Å). The phenyl rings are essentially planar, and the mean C–C distance (1.375 ± 0.005 Å) is normal. The dihedral angles between the two peripheral phenyl rings and the porphyrin core are 92.3 (2) and 64.5 (2)°. The geometry of the *p*-Me-TPP moiety (the average N–C_q, C_q–C_p, C_p–C_p, and C_q–C_m distances are 1.369 (9), 1.438 (5), 1.333 (7), and 1.399 (20) Å respectively)[18] is very similar to that found in other (tetraphenylporphinato)metal complexes.[16,19]

The electronic spectra of $[\mathrm{Os(TMP)(O)_2}]$ and $[\mathrm{Os(}p\text{-}\mathrm{X\text{-}TPP)(O)_2}]$ are distinctly different from that of $[\mathrm{Ru(TMP)(O)_2}]$. The osmium complexes show a three-band pattern at 580–590, 460–480, and 390–400 nm, as illustrated in Figure 3 for $[\mathrm{Os(TMP)(O)_2}]$. The visible spectrum of $[\mathrm{Ru(TMP)(O)_2}]$ features an intense band at 516 nm, and it resembles more closely the spectrum of $[\mathrm{Os(}p\text{-}\mathrm{X\text{-}TPP)(OR)_2}]$ (for example, $\mathrm{Os(TPP)(OEt)_2}$ λ/nm (log ϵ): 507 (4.07), 408 (5.02))[12] than that of $[\mathrm{Os(}p\text{-}\mathrm{X\text{-}TPP)(O)_2}]$. We offer no explanation for this difference, and future studies will be necessary to elucidate this point.

The reactivities of the $[\mathrm{Os(P)(O)_2}]$ complexes toward organic substrates have been investigated. At 20 °C, cyclohexene was not oxidized by $[\mathrm{Os(OEP)(O)_2}]$, $[\mathrm{Os(TPP)(O)_2}]$, and $[\mathrm{Os(TMP)(O)_2}]$, as neither cyclohexene oxide, cyclohexenone, nor cyclohexenol was formed after the reactions. With other organic substrates such as norbornene and benzyl alcohol, no detectable reaction was observed, even at 52 °C. When $[\mathrm{Os(TMP)(O)_2}]$ or $[\mathrm{Os(TPP)(O)_2}]$ was stirred with cyclohexene at 52 °C, cyclohexenol was formed. No cyclohexene oxide was found. The results are listed in Table VII. Since the reaction of $[\mathrm{Ru(TMP)(O)_2}]$ with cyclohexene yields cyclohexene oxide as one of the major products, the ruthenium and osmium complexes may react by different pathways. No catalytic aerobic oxidation of organic substrates has yet been observed with the $[\mathrm{Os(P)(O)_2}]$ complexes.

Acknowledgment. Financial support by the Department of Chemistry, University of Hong Kong, is gratefully acknowledged.

Registry No. *m*-CPBA, 937-14-4; $[\mathrm{Os(TMP)(O)_2}]$, 115076-43-2; $[\mathrm{Os(}p\text{-}\mathrm{MeO\text{-}TPP)(O)_2}]$, 115076-44-3; $[\mathrm{Os(}p\text{-}\mathrm{Me\text{-}TPP)(O)_2}]\cdot 2\mathrm{C_4H_8O}$, 115076-45-4; $[\mathrm{Os(TPP)(O)_2}]$, 110589-22-5; $[\mathrm{Os(}p\text{-}\mathrm{Cl\text{-}TPP)(O)_2}]$, 115076-46-5; $[\mathrm{Os(TMP)(CO)(EtOH)}]$, 115076-47-6; $[\mathrm{Os(}p\text{-}\mathrm{MeO\text{-}TPP)(CO)(EtOH)}]$, 115076-48-7; $[\mathrm{Os(}p\text{-}\mathrm{Me\text{-}TPP)(CO)(EtOH)}]$, 66082-87-9; $[\mathrm{Os(TPP)(CO)(EtOH)}]$, 115076-49-8; $[\mathrm{Os(}p\text{-}\mathrm{Cl\text{-}TPP)(CO)(EtOH)}]$, 115076-50-1; $[\mathrm{Os(OEP)(O)_2}]$, 51349-77-0; $[\mathrm{Os(OEP)(OH)_2}]$, 115092-12-1; cyclohexene, 110-83-8; cyclohexenol, 25512-63-4.

Supplementary Material Available: Tables of atomic and thermal parameters for hydrogen atoms, anisotropic thermal parameters, bond distances, and bond angles (4 pages); tables of calculated and observed structure factors (18 pages). Ordering information is given on any current masthead page.

---

(16) Che, C. M.; Lai, T. F.; Chung, W. C.; Schaefer, W. P.; Gray, H. B. *Inorg. Chem.* **1987**, *26*, 3907.

(17) Buchler, J. W.; LamKay, K.; Smith, P. D.; Scheidt, W. R.; Rupprecht, G. A.; Kenny, J. E. *J. Organomet. Chem.* **1976**, *110*, 109.

(18) The notation C_q, C_p, and C_m is that of: Hamor, T. A.; Caughey, W. S.; Hoard, J. L. *J. Am. Chem. Soc.* **1965**, *87*, 2305.

(19) See, for example: Ball, R. G.; Domazetis, G.; Dolphin, D.; James, B. R.; Trotter, J. *Inorg. Chem.* **1981**, *20*, 1556.

Contribution from the Department of Chemistry,
Polytechnic University, 333 Jay Street, Brooklyn, New York 11201

New Low-Temperature Synthesis of Transition-Metal Sulfides

Michael J. Martin,* Guo-Hua Qiang, and Donald M. Schleich

Received February 17, 1988

The reaction of hexamethyldisilthiane with transition-metal halides at room temperature results in the rapid synthesis of transition-metal sulfides. Sulfides that are normally difficult or even impossible to produce by using classical methods are readily produced. This method allows great control of reaction conditions and can be used with a wide range of transition metals and oxidation states. The sulfides that are synthesized are anhydrous, unlike those produced by many other low-temperature methods. This is a concern in applications such as the use of the materials as cathodes in secondary lithium batteries. The reactions were fast and usually exothermic, producing sulfides that were amorphous to X-ray diffraction. The only coproducts of the reaction between hexamethyldisilthiane and the metal halides are trimethylsilyl halides. These compounds are all volatile liquids and are easy to separate from the sulfides produced. Retention of the formal oxidation state of the metal from the halide was found in the sulfide in all cases.

Introduction

Transition-metal sulfides are of interest for many applications. Uses range from common ones such as dry lubrication to more specialized ones such as ionic intercalation for secondary batteries and catalysts.[1,2] The sulfides are well suited for these applications because of their physical structure as well as their chemical properties. Many of them, especially the dichalcogenides, have layered or sandwich-type structures.[1] These layers are bound to each other only by van der Waals forces, and therefore the layers can be easily pushed apart or slid alongside each other. The

---

(1) Rouxel, J.; Brec, R. *Annu. Rev. Mater. Sci.* **1986**, *16*, 137.

(2) Pohl, F. A.; Bohm, H. U.S. Patent 3 907 600, 1975.

0020-1669/88/1327-2804$01.50/0